The Journal of Antibiotics (2012) 65, 405–411

www.nature.com/ja

ORIGINAL ARTICLE

A novel acyclic oligomycin A derivative formed via retro-aldol rearrangement of oligomycin A

Lyudmila N Lysenkova[1], Konstantin F Turchin[1], Alexander M Korolev[1], Evgenyi E Bykov[1], Valery N Danilenko[2], Olga B Bekker[2], Alexey S Trenin[1], Sergei M Elizarov[3], Lyubov G Dezhenkova[1], Alexander A Shtil[4] and Maria N Preobrazhenskaya[1]

The antibiotic oligomycin A in the presence of K_2CO_3 and *n*-Bu_4NHSO_4 in chloroform in phase-transfer conditions afforded a novel derivative through the initial retro-aldol fragmentation of the *8,9* bond, followed by further transformation of the intermediate aldehyde. NMR, MS and quantum chemical calculations showed that the novel compound is the acyclic oligomycin A derivative, in which the *8,9* carbon bond is disrupted and two polyfunctional branches are connected with spiroketal moiety in positions C-23 and C-25. The tri-*O*-acetyl derivative of the novel derivative was prepared. The acyclic oligomycin A derivative retained the ability to induce apoptosis in tumor cells at low micromolar concentrations, whereas its antimicrobial potencies decreased substantially. The derivative virtually lost the inhibitory activity against F_0F_1 ATP synthase-containing proteoliposomes, strongly suggesting the existence of the target(s) beyond F_0F_1 ATP synthase that is important for the antitumor potency of oligomycin A.
The Journal of Antibiotics (2012) **65,** 405–411; doi:10.1038/ja.2012.38; published online 23 May 2012

Keywords: acyclic derivative of oligomycin A; apoptosis; F_0F_1 ATP synthase; oligomycin A; retro-aldol degradation; tumor cell lines

INTRODUCTION

The macrolide antibiotic oligomycin A (**1**) has long been considered a valuable experimental tool for studies of energy metabolism. The major pharmacological activity of **1** is the suppression of oxidative phosphorylation and a decrease of intracellular ATP content due to interaction with the oligomycin-sensitivity-conferring protein component of F_0F_1 ATP synthase.[1] These effects of **1** are of particular importance for the interference with ATP-dependent outward transport and the reversal of drug-resistant phenotypes in bacterial and mammalian cells.[2,3] Furthermore, growing interest in the mechanisms of energy disbalance in disease, to the most part (but not limited to) of cancer, opened the way to the application of **1** as a potent cytotoxic agent. Design of new compounds based on **1** scaffold is of interest, as F_0F_1 ATP synthase inhibitors are drug candidates for the treatment of bacterial infections and cancer.[4] Recently, we reported the modifications at the C_7 carbonyl group and the $C_2=C_3$ double bond of the antibiotic.[5] Search for rather selective methods of modifications of **1** prompted us to study the behavior of the molecule in the conditions of phase-transfer reactions.

RESULTS AND DISCUSSION

The reactions of **1** at elevated pH in many cases yielded a by-product that was difficult to isolate and identify. We found that this product can be obtained after column chromatography in 65% yield when **1** was stirred at room temperature with K_2CO_3 and *n*-Bu_4NHSO_4 in $CHCl_3$ in phase-transfer conditions. The HR-ESI-MS data revealed the molecular mass that corresponded to the product of dehydration of **1**. The 1D (^1H and ^{13}C) and 2D NMR correlation spectra (^1H–^1H COSY and ^1H–^{13}C HETCOR) showed a substantial change of the structure of novel compound compared with the parent **1**. Acetylation of novel compound with acetic anhydride in pyridine in the presence of 4-dimethylaminopyridine yielded the triacetate, for which the structure was confirmed by NMR and mass spectroscopy (Supplementary Table S1).

The biggest difference in ^1H and ^{13}C NMR spectra of **1** and the novel derivative was registered for the nuclei in the segment C_7–C_{12} and CH_3 groups bonded to the atoms of this segment: $C_{37}H_3$, $C_{38}H_3$ and $C_{39}H_3$ (Table 1). The difference in the C–C bonding, that is, the single bond in the segment C_7–C_{12} of **1** and the double bond of the same segment in the novel derivative, deserved a detailed investigation. The presence of the double bond C=C was supported by the following facts: (1) in ^1H NMR spectrum, the signal of one CH_3 group is shifted downfield to δ 1.679 p.p.m. in comparison with δ 1.01 p.p.m., the maximal value for $C_{37}H_3$, $C_{38}H_3$ or $C_{39}H_3$ in **1**; (2) the characteristic vicinal interaction ($J \sim 7$ Hz) for one CH–CH_3 group (as in **1**) is absent, whereas the splitting of the signal of this CH_3 group

[1]Gause Institute of New Antibiotics, Russian Academy of Medical Sciences, Moscow, Russian Federation; [2]Vavilov Institute of General Genetics, Russian Academy of Sciences, Moscow, Russian Federation; [3]Bach Institute of Biochemistry, Russian Academy of Sciences, Moscow, Russian Federation and [4]Blokhin Cancer Center, Russian Academy of Medical Sciences, Moscow, Russian Federation
Correspondence: Professor MN Preobrazhenskaya, Gause Institute of New Antibiotics, Russian Academy of Medical Sciences, 11 B Pirogovskaya Street, Moscow 119021, Russian Federation.
E-mail: mnp@space.ru
Received 26 December 2011; revised 4 April 2012; accepted 9 April 2012; published online 23 May 2012

Table 1 The ^{1}H and ^{13}C NMR spectra of 4a and 5

	4a			*5*		
No.	δ_C	δ_H	$J_{H,H}$	δ_C	δ_H	$J_{H,H}$
1	165.83 O–CO			165.33 C_q	—	
2	121.81 CH sp^2	5.86dd	15.6, 0.9	122.48 CH sp^2	5.84dd	15.7, 1.1
3	149.72 CH sp^2	6.73dd	15.6, 9.3	148.32 CH sp^2	6.78dd	15.7, 8.5
4	39.89 CH sp^3	2.41ddqd	9.3, 9.0, 6.7, 0.9	38.97 CH sp^3	2.59ddq	8.5, 7.9, 6.8
5	73.26 CH sp^3	3.75ddd	9.0, 2.6, 2.6[a]	74.60 CH sp^3	5.21dd	7.9, 4.8
6	47.44 CH sp^3	2.56dq	2.6, 7.2	47.58 CH sp^3	2.69qd	7.0, 4.8
7	216.62 CO	—		211.30 CO	—	
8	34.66 CH_2 sp^3	2.53dq, 2.41dq	18.1, 7.3	34.52 CH_2 sp^3	2.54, 2.38dq	18.1, 7.3
9	173.19 CH sp^2	8.00q	1.1	172.70 CH sp^2	7.94q	1.2
10	114.44 C_q sp^2	—		113.79 C_q sp^2	—	
11	208.25 CO	—		205.47 CO	—	
12	90.14 C_q sp^3	—		89.47 C_q sp^3	—	
13	75.90 CH sp^3	3.83dd	8.3[a], 1.6	75.48 CH sp^3	5.14d	1.8
14	33.62 CH sp^3	1.84dq	1.8, 6.9	33.26 CH sp^3	2.05m	
15	38.36 CH_2 sp^3	2.15m, 2.04m		38.26 CH_2 sp^3	2.07m, 1.83m	
16	129.45 CH sp^2	5.48dt	14.6, 7.3	129.00 CH sp^2	5.48ddd	14.5, 6.5, 8.0
17	132.61 CH sp^2	6.00ddt	14.6, 10.3, 1.1	132.55 CH sp^2	5.96dd	14.5, 10.3
18	129.94 CH sp^2	5.92dd	14.8, 10.3	130.10 CH sp^2	5.90dd	14.5, 10.3
19	137.24 CH sp^2	5.31dd	14.8, 8.8	136.91 CH sp^2	5.29dd	14.5, 8.7
20	44.51 CH sp^3	1.83m		44.66 CH sp^3	1.83m	
21	31.30 CH_2 sp^3	~1.40m		31.12 CH_2 sp^3	1.40m, 1.22m	
22	29.95 CH_2 sp^3	1.53m, 1.22m		27.61 CH_2 sp^3	1.40m, 1.20m	
23	69.40 CH sp^3	3.74ddd	8.0, 5.4, 2.0	69.27 CH sp^3	3.58ddd	7.7, 5.1, 2.2
24	35.34 CH sp^3	2.05m		35.21 CH sp^3	2.02m	
25	76.17 CH sp^3	4.97dd	11.4, 4.9	75.85 CH sp^3	5.00dd	11.4, 5.0
26	37.81 CH sp^3	1.75dq	11.4, 6.7	37.83 CH sp^3	1.72dq	11.4, 6.6
27	99.05 C_q sp^3	—		99.03 C_q sp^3	—	
28	25.85 CH_2 sp^3	1.88m, 1.22m		25.73 CH_2 sp^3	1.85m, 1.18m	
29	26.43 CH_2 sp^3	2.10m, 1.36m		26.23 CH_2 sp^3	2.05m, 1.36m	
30	30.36 CH sp^3	1.56m		30.00 CH sp^3	1.56m	
31	67.21 CH sp^3	3.97dt	10.3, 2.5	67.65 CH sp^3	3.72ddd	6.8, 6.0, 2.4
32	42.44 CH_2 sp^3	1.57m, 1.25m		39.70 CH_2 sp^3	1.55m (2 H)	
33	64.67 CH sp^3	4.00dqd	9.2, 6.2, 3.0	68.80 CH_2 sp^3	4.93tq	6.2, 6.2
34	24.56 CH_3 sp^3	1.202d	6.2	20.76 CH_3 sp^3	1.218d	6.2
35	16.43 CH_3 sp^3	1.146d	6.7	15.48 CH_3 sp^3	1.021d	6.8
36	9.36 CH_3 sp^3	1.095d	7.2	10.42 CH_3 sp^3	1.027d	7.0
37	7.48 CH_3 sp^3	1.016t	7.3	7.55 CH_3 sp^3	0.981t	7.2
38	5.15 CH_3 sp^3	1.679d	1.1	5.13 CH_3 sp^3	1.660d	1.2
39	19.61 CH_3 sp^3	1.320s		18.83 CH_3 sp^3	1.314s	
40	13.22 CH_3 sp^3	0.876d	7.0	14.09 CH_3 sp^3	0.948d	6.8
41	27.70 CH_2 sp^3	1.37m, 1.20m		30.08 CH_2 sp^3	1.40m, 1.22m	
42	11.62 CH_3 sp^3	0.797t	7.4	11.57 CH_3 sp^3	0.793t	7.4
43	5.53 CH_3 sp^3	0.805d	7.0	5.43 CH_3 sp^3	0.787d	7.0
44	11.63 CH_3 sp^3	0.922d	6.6	11.57 CH_3 sp^3	0.891d	6.8
45	11.13 CH_3 sp^3	0.872d	6.8	10.86 CH_3 sp^3	0.874d	7.0
				3 $COCH_3$ CO: 170.32, 170.17, 169.59		
				CH_3: 21.46, 20.57, 20.42		

[a]5-OH: δ 3.07, ^{3}J = 2.6 Hz; 13-OH: δ 2.12, ^{3}J = 8.3 Hz.

into the doublet ($J \sim 1.1$ Hz) is observed because of the interaction with CH=, typical for the interaction through four bonds in the system CH=CCH_3; (3) a low field position of this CH= signal (δ_H 8.00) presumes only sp^2 hybridization of the C atom. The *cis* orientation of H and CH_3 groups at the double bond C=C was supported by a rather high value of Overhauser effect $\eta_{CH=}\{CCH_3\} \approx 8\%$ measured by the increase of CH= signal after the saturation of the methyl signal of CH=C–CH_3. In ^{13}C NMR spectrum of the novel compound, these double bond carbons produced signals at δ 114.44 (C_q=) and 173.19 (CH=, $^{1}J_{CH}$ = 191.0

Hz as determined by satellites of ^{13}C in ^{1}H NMR spectrum). In the ^{1}H and ^{13}C spectra, there are signals of the ethyl group (absent in **1**) CH_2–CH_3 with big $|J_{gem}| = 18.0$ Hz between non-equivalent hydrogens of the CH_2 group.

The NMR and mass spectroscopy data corresponded to the two structures that might be formed through initial retro-aldol fragmentation of the *8,9* or *9,10* bond of **1**, leading to the formation of unstable intermediates **2a** or **2b**, respectively (Figure 1). Subsequent cyclization of each of these structures (leading to intermediates **3a** or **3b**) followed by dehydrogenation would produce compounds **4a** or **4b**. The NMR spectral data registered for the novel compound are in agreement with each of these structures. The assignment of the atoms in the fragment C_6–C_{12} of **1** can be done for both structures **4a** or **4b**. The 2D HMBC NMR spectrum allowed to select the structure **4a**, as the cross peaks were detectable in this spectrum, demonstrating the interaction through three bonds of one of ketone carbons with $C_{39}H_3$

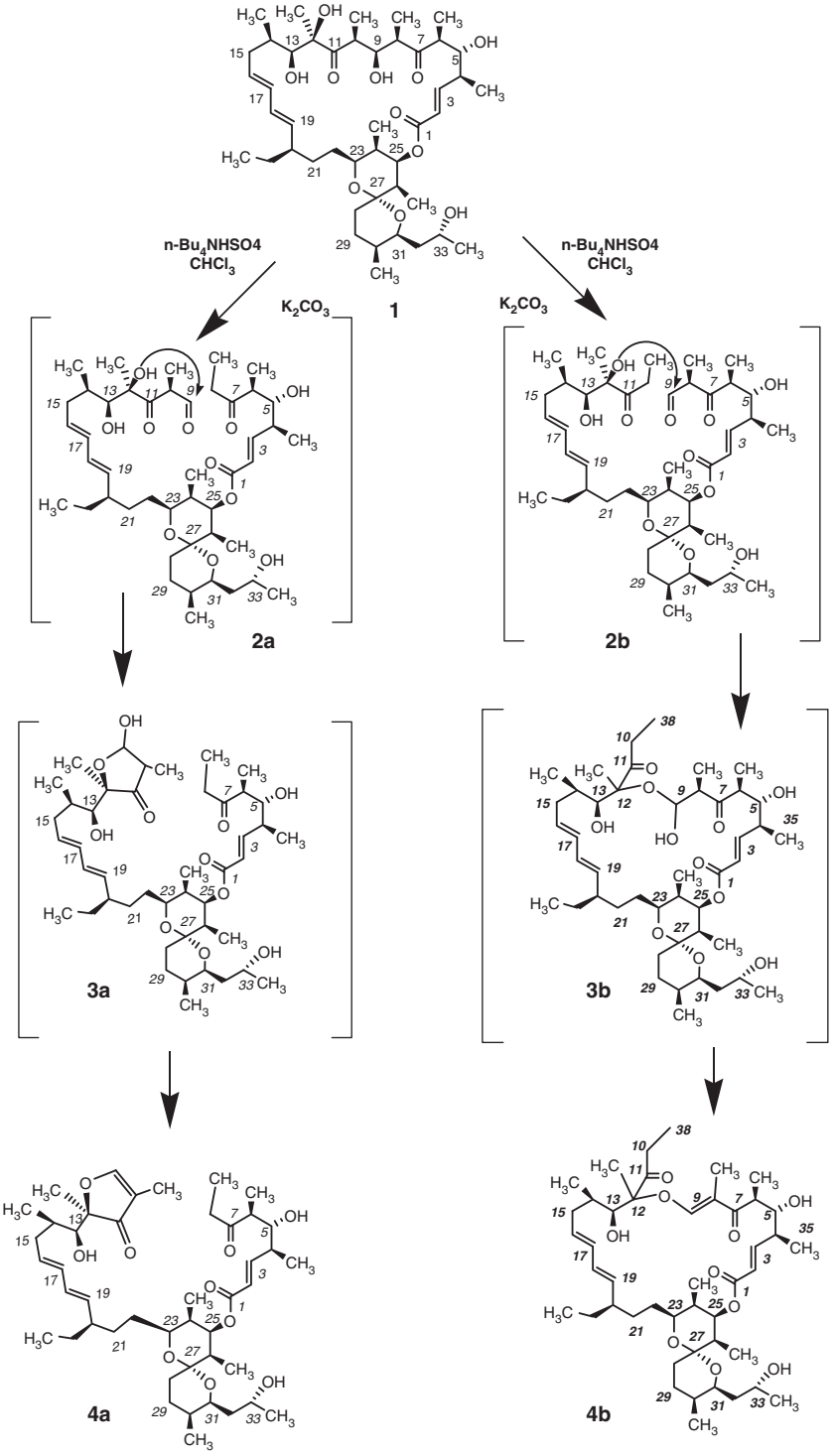

Figure 1 Degradation of oligomycin A in the conditions of alkaline phase-transfer reaction.

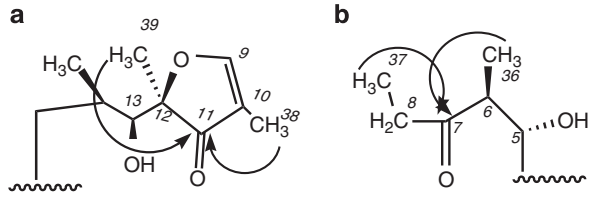

Figure 2 HMBC data for the fragment of compound **4a.** The arrows show observed cross peaks in HMBC 2D spectrum for the end fragments **a** and **b** of compound 4a.

(at C_{12}) and with CH_3 at the double bond (Figure 2a and b). Also, the cross peaks showed the interaction of another ketone carbon with $C_{36}H_3$ (at C_6) and with CH_3 of the novel ethyl group. These interactions are impossible in the structure **4b.**

Acetylation of **4a** by acetic anhydride in pyridine in the presence of 4-dimethylaminopyridine yielded tri-*O*-acetyl compound **5** in 86% yield (Figure 3, Table 1), whereas acetylation of **1** in similar conditions gave tetra-*O*-acetyl derivative **6**. The 5, 9, 13, 33-tetra-*O*-acetyl derivative **6** has been obtained previously by acetylation of **1** in the mixture of pyridine and acetic anhydride.[6] Compounds **5** and **6** differed mainly in the number of $COCH_3$ groups (3 and 4, respectively). Besides, in ^{1}H NMR spectrum of **6**, a broad signal at δ 3.29 (1H intensity) was present. According to the 2D COSY spectrum of **6**, the hydrogen exchanged with traces of water in the solvent ($CDCl_3$) and can be identified as 12-OH. This signal was absent in the spectrum of **5.** Thus, in both **5** and **6**, all hydroxyl groups at the secondary C atoms were acetylated, and the number of acetyl groups reflects different structures of **5** and **6**. All the above-mentioned peculiarities of ^{1}H and ^{13}C NMR spectra of **1** and **4a** were also detectable for triacetate **5** and tetraacetate **6**, further supporting the structures of **4a** and **5**. Thus, we obtained a novel acyclic derivative **4a** formed through the transformation of natural antibiotic **1**. NMR data for **6** are presented in Supplementary Information.

The structure of triacetate **5** was supported by tandem MS/MS spectra of this compound generated by ESI and collision-induced dissociation multiple reaction monitoring (MRM) mode; Figures 4 and 5). The fragmentation patterns of **5** depended on the collision energy applied for MS/MS fragmentation. With the increase of collision energy, smaller ions became prevalent in the mass spectra. The first product ion **a** mass spectra of **5** at low collision energies (55 eV) were dominated by *m/z* 861 ion, probably attributable to the loss of AcOH from the parent molecule. The second product ion fragments **b** at medium collision energies was observed at *m/z* 665, presumably arising from the loss of the substituted acrylic acid. The collision-induced dissociation spectra of **c** produced at 65 eV are attributable to the loss of AcOH during fragmentation of this anion. Possible structures of more abundant products of molecular ion (*m/z* 921) of **5** are depicted in Figure 4 and correspond to *m/z* 861 [921-AcOH] (**a**), *m/z* 665 (**b**), *m/z* 605 [665-AcOH] (**c**), and *m/z* 523 [605–Na-AcOH] (**d**). The most diagnostic is the fragment 665 (**b**), formed through the disruption of the C_{25}–O bond.

According to quantum chemical calculations by the Austin model 1 (AM1) method, ΔG_{298} of the cyclization reaction **2a→3a** to 15 kcal mol^{-1} is lower than ΔG_{298} of the cyclization reaction **2b→3b**. This may be explained by the fact that the closure of a 'small loop' on the path **2a→3a** is accompanied by an increase in entropy contribution (ΔS_{298}) by 43 kcal mol^{-1}, whereas the closure of a 'large cycle' on the path **2b→3b** is accompanied by a decreased entropy

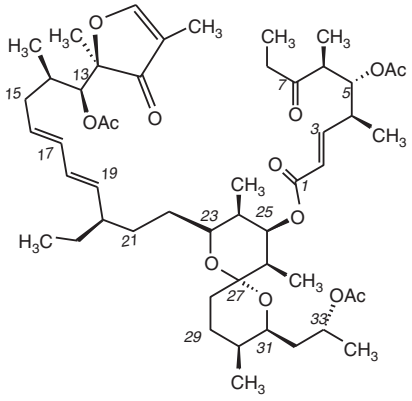

Figure 3 Triacetate of **4a** (**5**).

contribution (ΔS_{298}) by 17 kcal mol^{-1} (Table 2). Thus, the transformation **2a→3a** led to the compound, for which the molecule possesses a larger number of degrees of freedom. This suggests that the target reaction obeys the thermodynamic control.

Compound **4a** was generated through the initial retro-aldol fragmentation of the *8,9* bond. It is noteworthy that in this case, the retro-aldol degradation occurred under very mild conditions at room temperature, and the lactone bond was not hydrolyzed. It has been shown[7] that reflux of **1** in 1N methanolic NaOH resulted in a retro-aldol fragmentation of the *12,13* bond, and the newly formed aldehyde underwent further transformations. The hydrolysis of the lactone bond occurred, and the fragments of **1** formed in the course of numerous transformations were isolated and identified. Oligomycin C that is devoid of hydroxyl group in position 12,[8] underwent no transformation under the conditions in which **1** degraded.

A formazan conversion assay was used to determine the cytotoxic potencies of **1** and **4a** against the HCT116 human colon carcinoma and K562 leukemia cell lines. The 50% inhibitory concentration (IC_{50}) values of **1** were 1.0 ± 0.2 μM (for HCT116 cell line) and 0.2 ± 0.01 μM (for K562 cell line), whereas the respective values for **4a** were 3.1 ± 1.1 μM and 0.9 ± 0.1 μM. To get insight into the mechanism of cell death, we tested characteristic traits of apoptosis in K562 cells exposed to **1** and **4a**. As shown in Figure 6a, both **1** and **4a** caused an increase of the number of Annexin-V-positive cells and the loss of DNA integrity (sub-G1 peak events) as determined by flow cytometry. The percentages of Annexin-V-positive cells and the nuclei with fragmented DNA were similar for each compound (Figure 6a). These data indicate that **4a**, although being less potent than the parental **1**, retains the ability to trigger apoptosis in tumor cells at low micromolar concentrations.

Next, the potency of **1** and **4a** for bacterial cells was tested. Paper disks (7 mm in diameter) containing various amounts of tested compounds were applied on Petri dishes with logarithmically growing *Streptomyces fradiae* and incubated at 28 °C for 20 h. The halo diameters formed after the exposure of bacteria to **1** and **4a** were compared. At 0.001 nM per disk, compound **1** induced a zone of bacterial lysis 10 mm in diameter. In striking contrast, **4a** was two orders of magnitude less potent; a comparable size of the lytic zone was achievable with 0.1 nM per disk. A lower potency of **4a** for actinobacterial cells correlated with a decreased activity against filamentous fungi (molds). MICs were determined for yeast (*Candida albicans* ATCC 14053, *Cryptococcus humicolus* ATCC 9949) and fungal (*Aspergillus niger* ATCC 16404 and *Fusarium oxysporum* VKM F-140) strains after 24 or 48 h incubation, respectively, according to the

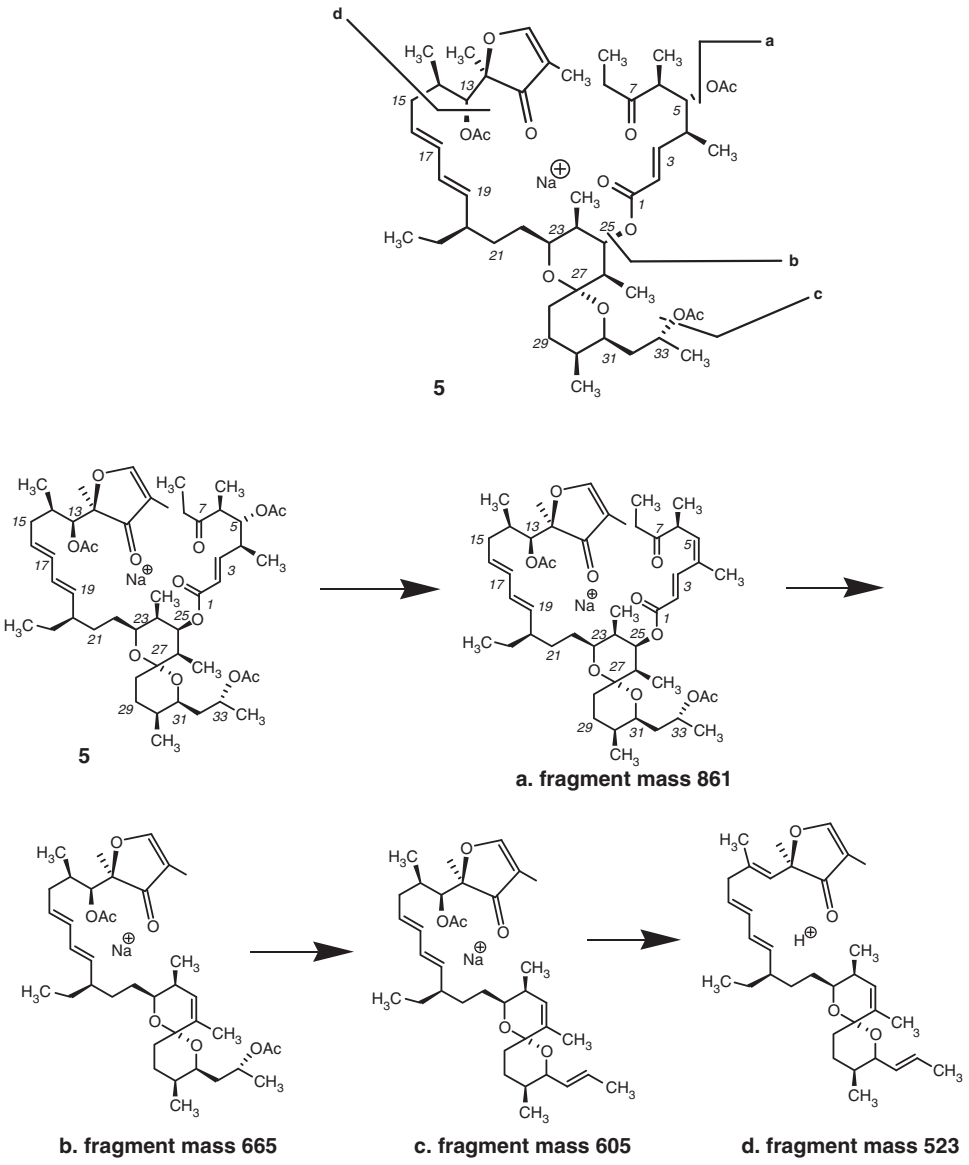

Figure 4 The fragmentation of **5** by ESI-MS/MS (MRM mode) at 65 eV.

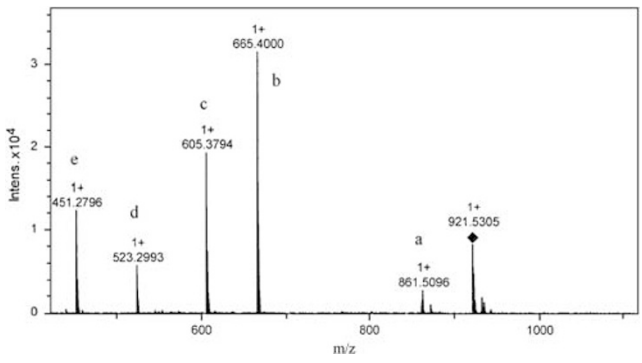

Figure 5 ESI-MS/MS spectrum of compound **5** generated by collision-induced dissociation (MRM mode) at 65 eV.

NCCLS, Standards M27-A and M38-A9.[9,10] As shown in Figures 6b, **1** was highly active against *Aspergillus niger* ATCC 16404 and *Fusarium oxysporum* VKM F-140 strains. The potency of **1** for these fungi was similar or even superior (for *Aspergillus niger*) to that of the reference drug amphothericin B. In contrast, the potencies of **4a** for both strains were substantially lower. The potencies of **1** and **4a** for yeast *Cryptococcus humicolus* ATCC 9949 were indistinguishable (Figure 6b).

A significantly lower inhibitory potency of **4a** than **1** for actinobacterial cell growth was further substantiated in a cell-free system, in which the ability of compounds to modulate F_0F_1 ATP synthase activity was tested (Figure 6c). The F_0F_1 ATP synthase-containing proteoliposomes were isolated from *Streptomyces fradiae* cells.[11]

Table 2 Thermochemistry parameters calculated by AM1 method

Thermochemistry parameters, kcal mol^{-1}	***2a***	***2b***	***3a***	***3b***
ΔH_{298}	765.40	765.78	771.14	768.77
ΔS_{298}	342.87	355.47	386.76	338.18
ΔG_{298}	663.18	659.80	655.83	667.56

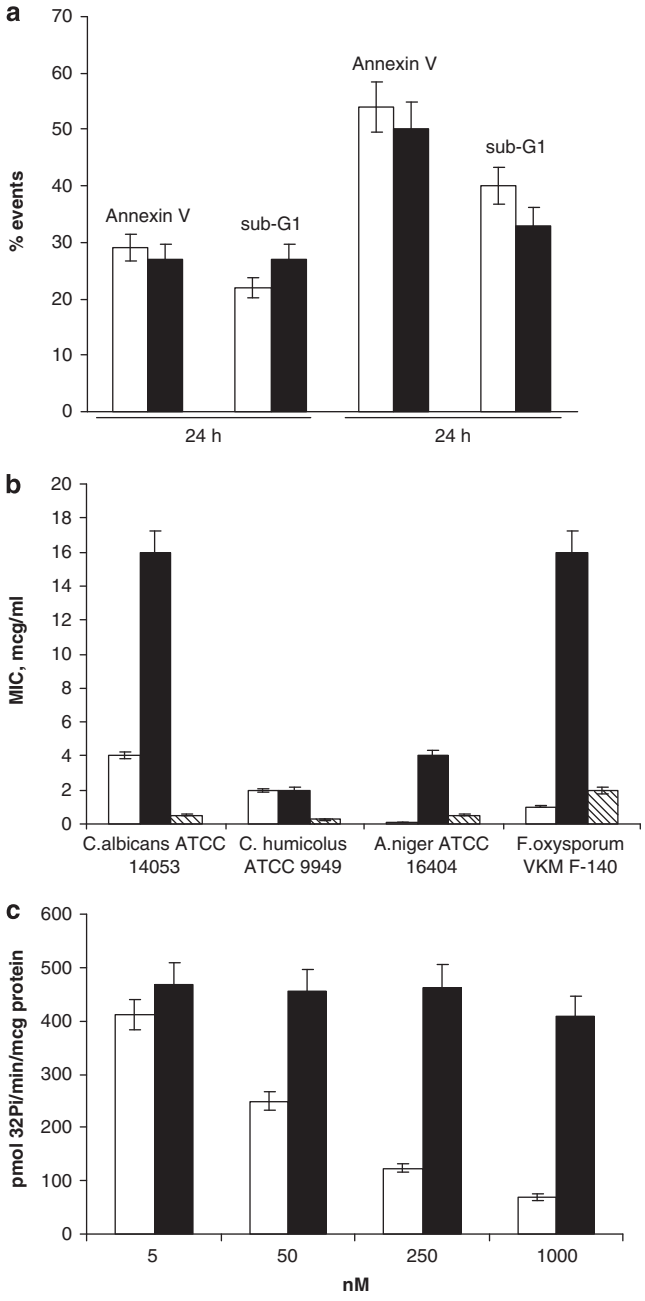

Figure 6 Effects of compounds **1** and **4a** on tumor and microbial cell viability and F_0F_1 ATP synthase activity.Open bars, compound 1; closed bars, compound 4a; hatched bars, amphothericin B (Amp). Data are mean ± s.d. of three independent experiments. (**a**) Apoptotic potency of **1** and **4a**. Values are percentages of drug-induced events (drug-treated K562 leukemia cells minus untreated counterparts) after treatment with $2 \times IC_{50}$ concentration of each compound, that is, 0.4 μM of **1** or 1.8 μM of **4a**. The percentages of Annexin-V-positive cells and subG-1 nuclei in untreated cells were within 10%. (**b**) Inhibition of yeast and fungal cell growth. (**c**) F_0F_1 ATP synthase activity in proteoliposomes.

Compound **4a** exerted no effect on proteoliposomal F_0F_1 ATP synthase activity at 1 μM (Figure 6c). These results are in agreement with a lower potency of **4a** in inhibiting the actinobacterial cell growth.

Finally, we studied the ability of **1** and **4a** to inhibit the growth of *Saccharomyces cerevisiae* S288C, the strain used for testing the sensitivity of yeast cells to **1**.[12] The minimal growth-inhibitory effect was detectable with 50 nM per disk of **1**, whereas **4a** caused no lysis of yeast cells, even at concentrations as high as 500 nM per disk.

Thus, the acyclic oligomycin A derivative **4a** retained the ability to induce apoptosis in tumor cells at low micromolar concentrations, whereas its antimicrobial potencies decreased substantially. Furthermore, **4a** virtually lost the inhibitory activity against F_0F_1 ATP synthase-containing proteoliposomes, strongly suggesting the existence of an additional target(s) beyond the F_0F_1 ATP synthase, which is important for the antitumor potency of **4a**. This hypothesis is in line with a complex mechanism of cytotoxicity of apoptolidin, a macrolide antibiotic structurally close to oligomycins.[13] Interestingly, a benzopyran analog BMS-199264 capable of selective inhibition of F_0F_1 ATP hydrolase but not F_0F_1 ATP synthase has been reported.[14,15] This switch of the enzymatic function was beneficial under the conditions of ischemia, because the drug reduced the ATP decrease during ischemia. Although the chemical structure of BMS-199264 is unrelated to oligomycins or apoptolidin, these findings raise the idea of the design of drugs that modulate particular functions of the complex energy-controlling machinery. From this viewpoint, the derivatives of **1** with a lower inhibitory potency against F_0F_1 ATP synthase deserve evaluation as tentative F_0F_1 ATP hydrolase antagonists.

EXPERIMENTAL PROCEDURES

Retro-aldol degradation of 1 and preparation of 4a

Oligomycin A (**1**; 0.2 g, 0.25 mmol) was dissolved in $CHCl_3$ (10 ml), then dry powdered K_2CO_3 and $(n\text{-}Bu)_4N^+HSO_4^-$ (0.03 g) were added under stirring, and stirring was prolonged for 48 h at room temperature. The reaction mixture was analyzed by TLC in toluene-EtOAc (3:1). Then, it was washed with water to pH 7.0, dried over Na_2SO_4, and concentrated. The reaction product was purified by column chromatography in toluene-EtOAc (3:1) to give 0.13 g (65%) of product of alkaline rearrangement **4a** as a colorless amorphous powder. MW was calculated for $C_{45}H_{72}O_{10}$ 772.5125. Found in ESI-mass spectrum 773.5188 $(M+H)$; 795.5018 $(M+Na)^+$; UV-spectrum, (λ_{max} nm, MeOH), (ε): 225 (20066), 270 (3633); IR ν max, cm^{-1} (film) 3452, 2965, 2934, 2880, 1704, 1698, 1651, 1615, 1455, 1380, 1278, 1223, 1188, 1136, 1093, 983; $[\alpha]_D^{20}$ −17.4 ^{0}(c 0.23 MeOH); R_t 14.01.

Synthesis of triacetate 5

To a stirred solution of **4a** (200 mg, 0.25 mmol) in pyridine (4 ml) 4-dimethylaminopyridine (80 mg, 0.65 mmol) and 0.5 ml Ac_2O were added. The reaction mixture was stirred for 48 h, and then analyzed by TLC in toluene-EtOAc (3:1). Then it was placed on ice, acidified by 1 N HCl until pH 3, and the reaction product was extracted with EtOAc. The extract was washed with water to pH 7, dried over Na_2SO_4, and concentrated. The reaction product was purified by column chromatography in toluene-EtOAc (3:1) to give 0.17 g (86%) of triacetate (**5**) as a colorless amorphous powder. MW was calculated for $C_{51}H_{78}O_{13}$ 898.5442. Found in ESI-mass spectrum (m/z) 921.2401 $(M+Na)^+$; UV-spectrum, (λ_{max} nm, MeOH), (ε): 217 (21767), 270 (4721); IR ν max, cm^{-1} (film) 2973, 2938, 2862, 1738, 1714, 1651, 1621, 1456, 1371, 1227, 1184, 1090, 1022, 983, 969; $[\alpha]_D^{20}$ -36.4^0 (0.33 MeOH); R_t 10.85.

Cytotoxicity of compounds 1 and 4a

The HCT116 colon carcinoma and K562 leukemia cell lines were purchased from ATCC (Manassas, VA, USA). Cells (5×10^3 in 190 μl of Dulbecco modified Eagle's medium supplemented with 5% fetal calf serum (HyClone, Logan, UT, USA), 2 mM L-glutamine, 100 U ml^{-1} penicillin, and 100 μg ml^{-1} streptomycin (all reagents and solvents were purchased from Sigma-Aldrich (St Louis, MO, USA), unless specified otherwise) were plated into a 96-well plate (Costar, Corning, NY, USA) and treated with 0.1% dimethyl sulfoxide (vehicle control) or with increasing concentrations of **1** or **4a** (each dose in triplicate) for 72 h at 37 °C, 5% CO_2. After the completion of drug exposure, 50 μg of 3-(4,5-dimethylthiazol-2-yl)-2,5-diphenyltetrazolium bromide was added into each well for an additional 2 h. Formazan was dissolved in

dimethyl sulfoxide, and the absorbance at $\lambda = 540$ nm was measured. Cell viability at a given drug concentration was calculated as the percentage of absorbance in wells with drug-treated cells to that of vehicle control cells (100%). The IC_{50} was defined as the concentration of the compound that inhibited cell viability by 50%.

Apoptotic death of K562 cells exposed to 1 and 4a

The K562 cells were plated on six-well plates (5×10^4 cells in 3 ml of culture medium). To ensure the damage of all cells in culture, each compound was tested at $\sim 2 \times IC_{50}$ concentration determined in the cytotoxicity tests (see above). The concentrations of **1** and **4a** are indicated in the legend to Figure 6. Cells were incubated for 24–48 h at 37 °C, 5% CO_2. The control wells contained no drug. After the completion of drug exposure, cells were washed with cold saline, harvested and divided into two portions. One aliquot of cells was stained with Annexin-V–fluorescein isothiocyanate as recommended by the manufacturer (Molecular Probes, Eugene, OR, USA). The second portion was lysed in the solution containing 0.1% sodium citrate, 0.3% NP-40, 50 μg ml^{-1} RNAse A and 10 μg ml^{-1} propidium iodide, and analyzed by flow cytometry on a FACSCanto II (Becton Dickinson, Franklin Lakes, NJ, USA) on FL2. The percentage of hypodiploid nuclei (a sub-G1 peak on histograms of cell cycle distribution) was calculated using the FACSDiva software (Becton Dickinson).

Modulation of F_0F_1 ATP synthase activity

The F_0F_1 ATP synthase-containing proteoliposomes were isolated from *Streptomyces fradiae* cells as described by us.[11] Briefly, 5 mg of total proteoliposomal protein was incubated with 2 mM [γ-^{32}P]ATP (10 imp min^{-1} pmol^{-1}; Phosphor, Moscow, Russia) in the buffer (50 mM Tris-HCl, pH 7.5; 1 mM $MgCl_2$, 10 mM $CaCl_2$, 50 mM NaCl, 1 mM 2-mercaptoethanol, 0.1 mM phenylmethylsulfonyl fluoride, 10% glycerol). Compounds **1** and **4a** were added to the reaction mixture 10 min before the addition of 'hot' ATP. The mixture was then incubated for 10 min at 37 °C, followed by the addition of 1 ml of 5% trichloroacetic acid, 5 mM 'cold' ATP and 2.5 mM Na_3PO_4. The acid-insoluble material was pelleted, then 0.5 ml of 5% trichloroacetic acid and 150 mg ml^{-1} of the activated carbon Norit A (Pharmacia Biotech, Uppsala, Sweden) were added to the supernatant for 60 min at 4 °C, followed by centrifugation. Radioactivity of the supernatant was counted by Cherenkov. A statistically significant inhibition of F_0F_1 ATP-synthase activity was detectable at 50 nM of **1**; a IC_{50} was ~200 nM.

ACKNOWLEDGEMENTS

We are very grateful to Dr Y Takahashi for critical analysis of the structure of the product of retro-aldol degradation of oligomycin A. Dr Takahashi's idea of the structure of compound **4a** has been confirmed by our HMBC and MS/MS data. This study was supported by the program 'Research and development of priorities of scientific and technological complex of Russia in 2007–2012' contract no. 02.512.12.2056, 2009, 'Development and validation of test systems for screening of oligomycin A derivatives', the grant of President of Russian Federation 'The Scientific School' 290.2010.4, and the grant of Russian Foundation for Basic Research 10-03-00210-a.

1 Hao, W., Chang, C. P., Tsao, C. C. & Xu, J. *J. Biol. Chem.* **285,** 12647–12654 (2010).
2 Li, Y.C., Fung, K.P., Kwok, T.T., Lee, C.Y., Suen, Y.K. & Kong, S.K. *Chemotherapy* **50,** 55–62 (2004).
3 Li, M., Chen, Z., Zhang, X., Song, Y., Wen, Y. & Li, J. *Bioresour. Technol* **101,** 9228–9235 (2010).
4 Salomon, A. R., Voehringer, D. W., Herzenberg, L. A. & Khosla, C. *Proc. Natl. Acad. Sci. USA* **97,** 14766–14771 (2000).
5 Lysenkova, L. N., Turchin, K. F., Danilenko, V. N., Korolev, A. M. & Preobrazhenskaya, M.N. *J. Antibiot.* **63,** 17–22 (2010).
6 Szilágui, L., Samu, J. & Harsanyi, I. *Spectr. Lett* **28,** 699–707 (1995).
7 Carter, G. T. *J. Org. Chem.* **51,** 4264–4271 (1986).
8 Szilágyi, L. & Fehér, K. *J. Mol. Struct* **471,** 195–207 (1998).
9 National Committee for Clinical Laboratory Standards *Reference method for broth dilution antifungal susceptibility testing of yeasts. Approved standard M27-A* (National Committee for Clinical Laboratory Standards, Wayne, PA, USA, 1997).
10 National Committee for Clinical Laboratory Standards *Reference method for broth dilution antifungal susceptibility testing of conidium-forming filamentous fungi. Approved Standard M38-A. NCCLS* (National Committee for Clinical Laboratory Standards, Wayne, PA, USA, 2002).
11 Alekseeva, M. G., Elizarov, S. M., Bekker, O. B., Lubimova, I. K. & Danilenko, V. N. *Biochem. Mosc. Suppl. A Membr. Cell* **26,** 41–49 (2009).
12 John, U. P. & Nagley, P. *FEBS Lett.* **207,** 79–83 (1986).
13 Wender, P. A., Jankowski, O. D., Longcore, K., Tabet, E. A., Seto, H. & Tomikawa, T. *Org. Lett.* **8,** 589–592 (2006).
14 Atwal, K. S., Wang, P., Rogers, W. L., Sleph, P., Monshizadegan, H. & Ferrara, F. N. *et al. J. Med. Chem.* **47,** 1081–1084 (2004).
15 Grover, G. J., Marone, P. A., Koetzner, L. & Seto-Young, D. *Int. J. Biochem. Cell Biol.* **40,** 2698–2701 (2008).

Supplementary Information accompanies the paper on The Journal of Antibiotics website (http://www.nature.com/ja)